Benthic Ba fluxes in the central Equatorial Pacific, implications for the oceanic Ba cycle

Adina Paytan [*], Miriam Kastner

Scripps Institution of Oceanography, University of California, San Diego, La Jolla, CA 92093-0212, USA

Abstract

High resolution pore-water dissolved Ba concentration–depth profiles were determined at seven sites across an Equatorial Pacific productivity gradient from 12°S to 9°N, at 140°W. These data are important for understanding the physical, chemical, and biological controls on Ba recycling in the ocean, and for evaluating the paleo-oceanographic significance of Ba content in central Equatorial Pacific sediments.

Pore-water Ba concentrations at all sites are higher than in the overlying bottom water, leading to a diffusive flux of Ba into the ocean. A pronounced subsurface concentration maximum exceeding barite solubility characterizes the dissolved Ba pore-water profiles, suggesting that the Ba regenerated in the upper few millimeters of sediment is not controlled by barite solubility. A few centimeters down-core Ba concentrations reach a relatively constant value of approximately barite saturation.

The benthic Ba flux shows a clear zonal trend, with a maximum between 2°S and 2°N, most probably due to higher productivity at the equatorial divergence zone, and with lowest values at the southern and northern extremes of the transect. The dissolved Ba flux between 2°S and 2°N is ~ 30 nmol cm^{-2} yr^{-1} and drops to 6 nmol cm^{-2} yr^{-1} at 12°S. Even the lowest fluxes are significantly higher than those previously reported for the open ocean. In the Equatorial Pacific the calculated Ba recycling efficiency is about 70%. Thus, $\sim 30\%$ of the particulate Ba flux to the deep ocean is preserved in the sediments, compared with less than 1% for organic carbon and $\sim 5\%$ for biogenic silica.

Mass balance calculation of the oceanic Ba cycle, using a two-box model, implies benthic Ba fluxes similar to those reported here for a steady-state ocean.

Keywords: Equatorial Pacific; barium; geochemical profiles; mass balance; geochemical cycle

1. Introduction

Barium concentrations of seawater and marine sediments have been recently employed as proxies for a variety of paleo-oceanographic processes. Examples include: the reconstruction of changes in oceanic circulation through glacial interglacial transitions utilizing Ba/Ca ratios in foraminifera [1]; the assessment of changes in upwelling conditions by measuring fluctuations of Ba/Ca ratios in corals [2]; the estimation of paleoproductivity from Ba concentrations in sediments [3–5]; and evaluation of organic carbon exported from the euphotic zone, using suspended particulate barite in the water column

* Corresponding author. Tel.: (619) 534 1826. Fax: (619) 534 0784. E-mail: apaytan@ucsd.edu

[6,7]. The Sr isotope composition of marine barite has also been shown to be a reliable recorder of the seawater Sr isotopic ratio [8]. In order to rigorously utilize Ba for such studies a better understanding of the biogeochemical behavior of this element, especially during early diagenesis, is required. The phases involved, recycling rates, and burial efficiencies of Ba in sediments are not well defined, as yet. Also, the benthic Ba flux and its relation to upper water column processes such as biological productivity and particulate flux are not well known. These questions were addressed by analyzing pore-water and sediment Ba concentrations and calculating benthic Ba fluxes along a south–north transect from 12°S to 9°N in the Equatorial Pacific, at 140°W ~ 4300 m water depth. The transect is situated in a region of importance to global climate [9] and is characterized by a prominent productivity gradient [10].

Although the distribution of dissolved Ba in seawater has been determined (GEOSECS expeditions [11–13]), little is known about its biogeochemistry or reactivity during early diagenesis. Dissolved Ba in the open ocean is generally depleted in surface waters and enriched in deep waters, with increasing concentration along deep water advective flow lines [11–13]. Such concentration profiles indicate involvement in biological processes. This concept is supported by the observation that dissolved Ba concentrations in the water column positively correlate with those of silica and alkalinity [13,14]. The particulate Ba flux correlates well with the particulate organic carbon flux and with the biological productivity of the overlying water [5,7,15]. The oceanic distribution of dissolved Ba is most likely controlled by uptake of Ba in the upper water column, where biological activity is intense, and by regeneration at depth [16,17]. Benthic regeneration flux calculations presented here suggest that a significant fraction of the particulate Ba flux is remobilized within the first few millimeters of the sediment after burial, resulting in a substantial benthic flux of Ba into the ocean.

The particulate Ba flux to the deep ocean in the Equatorial Pacific ranges between 7 and 40 nmol cm^{-2} yr^{-1} and correlates positively with the organic carbon flux [15]. The principal carrier of Ba in these particles has been suggested to be a Sr-enriched barite $((Ba,Sr)SO_4))$ [18]. The exact mechanism of its formation is not fully understood, but Bishop [6] and Bernstein [19] have suggested that barite precipitates in micro-environments containing decaying organic matter, acantharian shells and/or other biogenic remains. Biological mediation or micro-environmental precipitation is essential because the water column is undersaturated with respect to barite at all depths [20,21]. Dissolved Ba profiles suggest that some of the newly formed barite dissolves at depth in the water column but, because of the low solubility of barite and the fact that much of what reaches the sea floor does so within fecal pellets, we assume that the majority of the barite formed reaches the sediment.

Estimates of benthic Ba fluxes have been made for a number of suboxic sediments [22,23], but such sediments constitute only a small fraction of the sea floor. Oxic sediments dominate the pelagic environment, therefore, a better understanding of the biogeochemistry and oceanic cycling of Ba in the pelagic environment is essential for developing and applying Ba as a tool for geochemical and paleo-oceanographic studies. This study examines the early diagenesis of phases containing Ba in oxic sediments along a productivity gradient and evaluates the impact of this process on the chemical cycle of Ba in the ocean.

2. Experimental

2.1. Sampling location and procedures

Pore-waters were extracted from the upper ~ 30 cm of sediments along an Equatorial Pacific transect at 140°W, from 12°S to 9°N, at a water depth of approximately 4300 m (JGOFS–EqPac, Leg TT013, November 1992), sample locations and water depths are listed in Table 1. Sediments were collected using a multi-corer. All cores had a well-preserved sediment–water interface with an occasional fluff of phyto-detritus, overlain by clear bottom seawater. Thus, sediment disturbance seems to have been minimal during the coring and recovery operations. Sub-cores were transferred within minutes of arrival on board into a cold room of 2°C, where they were sectioned into 0.5, 1 and 2 cm intervals in a nitrogen atmosphere glove bag, and centrifuged at 7000–10,000 rpm. The pore-waters obtained were passed

Table 1
Cores analyzed for pore-water Ba concentrations

Core number	Latitude	Longitude	Water depth (m)
12S-03-A	11°59'S	134°57'W	4282
2S-10-B	12°00'S	134°57'W	4280
5S-07-A	4°58'S	139°44'W	4256
5S-05-B	4°58'S	139°44'W	4263
2S-03-A	1°52'S	139°42'W	4376
2S-04-B	1°51'S	139°43'W	4393
0-02-A	0°60'N	139°45'W	4315
0-04-B	0°06'N	139°43'W	4301
2N-08-A	2°30'N	140°55'W	4412
2N-08-B	2°37'N	140°80'W	4413
5N-04-A	5°47'N	139°83'W	4416
5N-01-B	5°42'N	139°38'W	4422
9N-06-A	8°55'N	139°51'W	4992
9N-06-B	8°55'N	139°52'W	4994

through pre-washed Nucleopore 0.45 μm filters in a nitrogen atmosphere, acidified to a pH of 2 with distilled HNO_3, and stored in acid-cleaned polypropylene bottles at 2°C. The pore-water sampling procedure was usually completed within less than 24 h of core recovery. Two cores from each latitude were processed in order to identify spatial variability. All the equipment used for sample processing was thoroughly pre-cleaned with 8 N HNO_3, in order to reduce the blank.

2.2. Analytical methods

Ba concentrations were measured using isotope dilution inductively coupled plasma mass spectrometry (ID–ICP–MS). Approximately 1 g of solution was weighed and a ^{135}Ba spike was added to produce a ratio of ^{138}Ba/^{135}Ba between 0.7 and 1.2. Each sample was diluted 50 fold with 0.1 M distilled HNO_3. The ^{135}Ba spike was prepared from $BaCO_3$ (Oak Ridge #000513-77-9) in 2 N distilled HNO_3. The spike solution was calibrated several times by thermal ionization mass spectrometry (by G. Lugmair) and yielded a ^{135}Ba concentration of 5.6035 × 10^{-10} mol g^{-1} and a ^{138}Ba/^{135}Ba ratio of 0.039900 ± 5. Uncertainties in calculated Ba concentrations associated with the determination of the spike composition are at least two orders of magnitude less than those associated with the reproducibility of the ICP–MS.

The ^{138}Ba/^{135}Ba ratios of the spiked samples were determined on a VG Plasma Quad ICP–MS. The signal to noise ratio for all analyses was greater than 100. Between samples, a 3% HCl solution was aspirated until the monitored Ba masses matched machine noise levels. The blank was estimated by carrying both the overlying seawater from each core and doubly distilled water through the extraction and spiking procedures, as well as through the ICP analysis. The results of these measurements agree with published deep-water dissolved Ba concentrations in the vicinity of the sampling locations [11–13], and the distilled water blanks were indistinguishable from the ICP–MS background level. A gravimetric Ba standard, with a Ba concentration in the range of the pore-water samples, was prepared and spiked identically. This standard was interspersed through the samples to monitor instrument offsets and drift, and to correct for machine mass bias [24]. The ^{138}Ba/^{135}Ba ratio of each sample was adjusted by the deviation of the measured ratio of the standard from the actual ratio in order to ensure accuracy and monitor reproducibility. Based on repeated analyses of the standard and samples over several runs, on different days, the 2σ error in the ICP analyses is estimated at ±2%.

3. Results and discussion

3.1. Pore-water Ba concentrations

Pore-water dissolved barium concentrations determined in this study are given in Table 2 and Fig. 1. As seen in Fig. 1, all pore-water Ba concentrations are higher than those of the overlying seawater, resulting in a diffusive flux of Ba out of the sediment. A high subsurface Ba concentration maximum is observed at all stations, except at 12°S. Such maxima have also been observed for dissolved Mo and Re concentrations (D. Colodner, pers. commun.) in these cores, and for dissolved Cu concentrations in other cores from this area [25]. Pore-water subsurface Ba concentration maxima have been observed in the Gulf of California [26] and in the Southern Ocean [27]. Similar subsurface maxima of nitrate and ammonia were, however, regarded as sampling arti-

facts [28,29]. Notwithstanding that the presumed processes responsible for these nitrate and ammonia fictitious maxima are less likely to produce similar Ba concentration maxima, the observation that, regardless of the time span between core recovery and processing of each of the seven sets of duplicate cores, the Ba concentration maxima are the same, suggests that these maxima, shown in Fig. 1, are real and representative of in situ Ba production. Furthermore, the consistency between the Ba fluxes obtained from the pore water profiles, the benthic chambers obtained by McManus et al., and derived

from oxygen flux information, discussed below, further strengthens this conclusion. The highest dissolved Ba concentration at each site occurs in the top few millimeters of the sediment (0–0.5 cm interval of sampling), and decreases down-core within a few centimeters of burial, reaching an essentially constant value (typically at 1–2 cm below surface). These results indicate that Ba is being regenerated in the upper few millimeters of the sediment, where maximum remineralization of organic matter and other biogenic compounds occurs.

The concentrations of dissolved Ba at the subsur-

Table 2

Pore-water Ba concentrations (nmol kg^{-1}) at 7 stations along the JGOFS–EqPac transect

Depth (cm)	12°S A	12°S B	5°S A	5°S B	2°S A	2°S B	0° A	0° B	2°N A	2°N B	5°N A	5°N B	9°N A	9°N B
Bottom water	117	120	125	121	137	130	141	146	141	145	150	149	145	150
0.25	167	172	312	253	412	382	437	426	363	382	300	326	285	252
0.75	196		285	226	234	257	298	295		351	239	215	177	176
1.5	163		195	200	222	242	295	264	315	267	245	221	174	185
2.5	178	179	201	199	257	255	286	268	298	291	240	237	186	183
3.5	181	185	200	196	263	275	295	296	302	285	241	228	187	199
4.5	193	186	210	208	274	259	282	268	323	295	243	228	193	226
5.5								249						
6.0	197	195	226	205	273	263	264		274	300	254	244	211	211
7.0								307						
8.0	217	211	211	200	276	251	310		282	293	253	234		199
9.0								235						
10.0			201	199	291	247	235			282	258	227		204
11.0	212	209						250						
12.0			200	201	280	252	236		260		270	253	219	221
13.0								232						
14.0			194	193	271	233	241			302				
15.0	209	207							283			217	218	222
16.0					310	275		229						
17.0			195	202			250							
18.0									251	288		215	219	224
19.0	214	212						279						
20.0					230	220					231			
21.0							231		263	277			210	213
22.0			193	195				240						
23.0	213	205												
24.0					247	233			230	281	227		203	
25.0														
26.0								238						
27.0	207	207	192											
28.0					235									

Uncertainties are ±2% (2σ). The depth in centimeters represents the middle point of the sample interval. A and B represent two distinct cores at each site.

face maxima are supersaturated with respect to barite by at least 40% at the equator [19–21,30,31], indicating that barite solubility does not control the release of Ba at these depths. The pore-water Ba concentration maxima must be sustained by its rapid release from reactive phases that carry Ba to the sediment; production rates of dissolved Ba must exceed bioturbation rates. Calculations based on the steady-state diagenetic equation of Berner [32] indicate that the Ba production rates exceed bioturbation rates obtained from ^{14}C and ^{210}Pb measurements in these cores [33,34]. The calculated production rates are, however, somewhat lower than the rain rate of particulate Ba at these sites [15]. The most likely sources of the reactive Ba are labile organic matter, adsorbed Ba, and/or a celestite–barite solid solution phase. Although barite is the principal carrier of Ba to the sediment [6,17], the barite that precipitates in the water column is thought to be poorly crystalline and to have variable and relatively high Sr contents [18,22]. Celestite is substantially more soluble than barite and Sr substitution in barite increases its solubility and dissolution rate. The pore-water Ba concentration data do not provide sufficient information for assessing the controlling mechanism of Ba production responsible for the subsurface Ba concentration maxima, shown in Fig. 1.

3.2. Calculations of benthic Ba fluxes

The Ba flux into the ocean at each station was calculated using Fick's first law modified for sediments, expressed as:

$$J_s = \phi D_s \left[\frac{\partial c}{\partial z} \right]_{z=0} \qquad (1)$$

where J_s represents the flux out of the sediment (in nmol cm^{-2} yr^{-1}); ϕ stands for the sediment porosity (which is dimensionless); D_s refers to the diffusion coefficient in the sediment (in cm^2 sec^{-1}); and $\partial c/\partial z$ is the concentration gradient between the pore-water maxima and bottom water (in nmol cm^{-3} of pore-water Ba per centimeter in the sediment (nmol cm$_{pw}^{-3}$ cm$_{sed}^{-1}$)). The sediment porosities (ϕ) were determined on sample splits from the same cores as described in McManus et al. [35]. The sediment diffusion coefficient (D_s) for Ba was calculated using:

$$D_s = D_m \phi^{1.6} \qquad (2)$$

where D_m denotes the molecular diffusion coefficient of Ba in solution, which is equal to 4.04×10^{-6} cm^2 sec^{-1} at bottom water temperatures of 2°C [36], and ϕ is the mean porosity in the top 0.5 cm of the sediment in each core. The exponential of 1.6 in Eq.
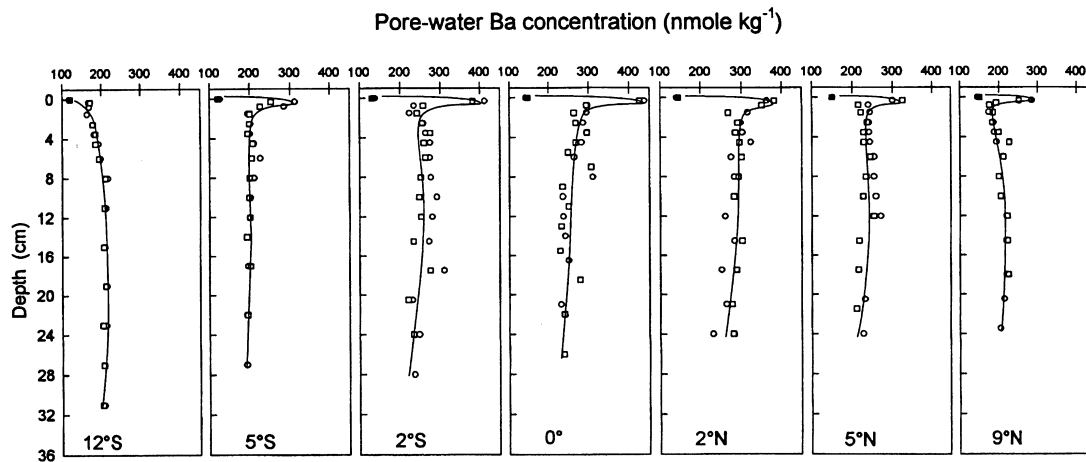
Pore-water Ba concentration (nmole kg^{-1})

Fig. 1. Pore water barium concentrations (nmol kg^{-1}) versus depth along the 140°W EqPac transect. Symbols indicate data from cores A (○) and B (□) collected at each latitude. The solid symbols represent bottom water concentrations.

(2) was chosen by McManus et al. [35] for these sediments, based on their porosity data and the empirical relations between porosity and tortuosity by Berner [32]. The value of the exponential is comparable to that derived empirically in this same area ($D_s = D_m \phi^{1.7}$) by Martin et al. [37] using conductivity measurements for sediments.

Benthic fluxes are best measured in situ at the sediment–water interface, however, pore-water gradients may also be used to estimate benthic fluxes, provided high resolution accurate concentration measurements are available. In this study, pore-water diffusive fluxes of Ba were estimated assuming linear gradients between bottom water and near surface pore-water concentration maxima. A sampling resolution of 0.5 cm in the upper interval may miss a sharper gradient that may be present. Therefore, some of the estimated fluxes reported here may represent lower than maximum values. Fluxes calculated in this manner are susceptible to uncertainties resulting from sediment disturbance as well as temperature and pressure changes encountered during core recovery [38,39]. In the present study only cores in which the sediments appeared to be undisturbed were used, blanks were closely monitored and cores were maintained at bottom water temperature. The decrease in hydrostatic pressure as cores are brought to the surface from a few kilometer depths causes pore-water displacement, which alters pore-water gradients within the upper few millimeters of the sediment [40,41], leading to uncertainties in estimates of regeneration fluxes. Such artifacts caused by core decompression were found empirically, by comparing in situ harpoon samples and ship-board pore-water samples, and calculated theoretically [40,41]. To evaluate this effect, two estimates of the Ba benthic flux were made for each site, one assuming no pore-water displacement (i.e. a linear gradient from the Ba concentration of bottom water to that at the Ba maximum at 0.3 cm down-core), and a second assuming that the pore-water was displaced 5 mm upwards during recovery relative to the sediment surface (e.g., the Ba concentration measured at 0.3 cm was presumed to correspond to 0.8 cm in situ subsurface depth); this amount of upward displacement was observed by Jahnke et al. [40] for similar sediment cores at about 4 km water depth. The actual depth of the measured dissolved Ba concentration

maximum may occur anywhere within the upper sampling interval of 0–0.5 cm; 0.3 cm was chosen arbitrarily as the depth of the maxima. The depth of 0.8 cm used for the second calculation, which assumes that the measured depth of the maxima is at 0.3 cm and takes into account the hydrostatic pressure effect, could actually be situated at 0.5–1 cm subsurface depth.

The uncertainties arising from the use of a constant porosity value in the uppermost 0.5 cm interval and assigning the maxima depth at 0.3 cm may be as high as ±30% for the maximum flux calculations and ±15% for the minimum flux calculations. These uncertainties are based on flux calculations made by shifting the depth of the maximum by ±0.1 cm relative to 0.3 and 0.8 cm. This is significantly larger than the analytical reproducibility of the Ba concentration measurements or the uncertainty in the diffusion coefficient ($\pm 0.5 \times 10^{-6}$ cm^2 sec^{-1}, [36]). Resulting flux estimates and associated uncertainties are given in Table 3. In the table, unadjusted estimates represent maximum fluxes and adjusted estimates represent minimum fluxes. Calculated maximum and minimum estimates differ by up to a factor

Table 3
Benthic flux of dissolved Ba (nmol cm^{-2} yr^{-1}) calculated from Eq. (3) for sediments along the JGOFS-EqPac transect

Core number	Porosity [a]	Maximum flux [b] ±30%	Minimum flux [c] ±15%
12-S-03-A	0.89	16	6
12-S-10-B	0.89	16	6
5-S-07-A	0.78	42	16
5-S-05-B	0.80	31	12
2-S-03-A	0.86	79	29
2-S-04-B	0.87	74	28
0 -02-A	0.85	106	40
0 -04-B	0.86	101	38
2-N-08-A	0.87	65	25
2-N-08-B	0.86	67	25
5-N-04-A	0.81	37	14
5-N-01-B	0.81	43	16
9-N-06-A	0.90	44	16
9-N-06-B	0.90	32	12

[a] Mean porosity in the upper 0.5 cm of sediment [35]. [b] Ba flux calculated using a linear gradient from the sediment–water interface to 0.3 cm. [c] Ba flux calculated after correction for water expansion using a linear gradient from the sediment–water interface to 0.8 cm.
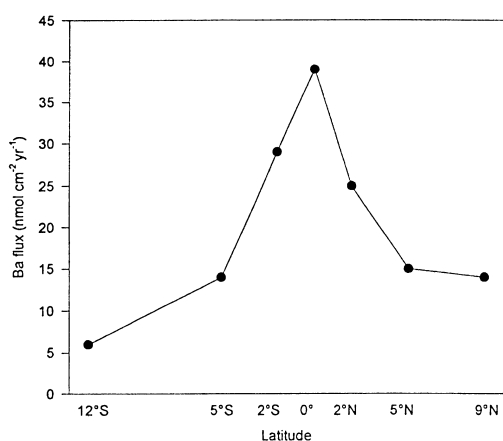
Fig. 2. Geographical distribution of benthic Ba fluxes at 140°W.

of 2.5. Preliminary benthic Ba flux estimates, made concurrently using a free vehicle benthic lander, are between 5 and 30 nmol cm^{-2} yr^{-1} for the different stations (McManus pers. commun.). These values are consistent with the calculated minimum fluxes in Table 3, suggesting that the effect of displacement due to decrease in hydrostatic pressure upon core recovery must not be neglected. If, however, the uncorrected maximum flux estimates obtained here are assumed to be accurate values, an explanation of the significant discrepancy between the in situ measurements and the ship board pore-water data and flux calculations would be required. The lower flux calculations are used in the discussion below. It is suggested that fluxes derived from careful high-resolution pore-water concentration studies at in situ temperatures, when corrected for pressure displacement effects, are compatible with those acquired in situ, thus could be reliably used for regeneration and benthic flux studies. Fig. 2 shows the latitudinal distribution of the above fluxes corrected for hydrostatic pressure displacement.

Notwithstanding the fairly large range in Ba fluxes shown in Table 3, several important conclusions can be drawn. The pore-water Ba fluxes estimated in this study are considerably higher than those previously estimated for Ba in the pelagic environment. In part, this discrepancy results from the paucity of similar high resolution data; coarser sampling intervals were

used in previous studies [21,42]. Benthic dissolved Ba fluxes of similar magnitude were previously reported only from suboxic sediments [22,23,26]. This study indicates that high benthic fluxes of dissolved Ba also occur in sediments underlying areas of high productivity in the pelagic environment. Such high Ba fluxes and recycling efficiencies are, however, required to maintain steady-state conditions in the ocean, assuming the regeneration occurs in the sediment [11,42].

The benthic dissolved Ba fluxes calculated in the present study show clear zonal trends, with a maximum at the equator and with the lowest values occurring at the southern and northern extremes of the transect. As expected from the good correlation between particulate organic carbon and particulate Ba fluxes observed in the water column [5,15], this spatial Ba benthic flux distribution (Fig. 2) reflects the productivity of the overlying water column, which is highest along the equatorial divergence zone [10]. This distribution of pore-water Ba fluxes about the equator is consistent with that of other benthic fluxes obtained along this transect, that is, of dissolved silica [35], nitrate, phosphate, alkalinity, oxygen [29], and of organic carbon [37]. Macrofauna and bacteria are also more abundant and show maxima in activity in the near-surface layer of the sediment around the equator [33,43].

As an independent check on the Ba regeneration fluxes calculated from pore-water data, an estimate of this flux was made using the oxygen consumption rates in these sediments and the Ba to organic carbon ratio of particulate matter arriving at the sediment. The calculations assume a Redfield O/C ratio of 1.3, a Ba to organic carbon ratio of particulate rain of 0.02 [15], and a negligible difference in the diffusion coefficients of oxygen and Ba. Using measured oxygen consumption rates of 0.7–0.8 mmol m^{-2} day^{-1} for stations around the equator and 0.2 mmol m^{-2} day^{-1} at 12°S [29], the calculated Ba fluxes from the sediments are 34–54 and 9.5 nmol cm^{-2} yr^{-1}, respectively, for nearest and furthest stations from the equator. These values are well within the range of the minimum fluxes calculated from the pore-water profiles (Table 3). The agreement between these two independent calculations suggests that the amount of Ba released near the sediment–water interface is in line with that calculated by the

decomposition of particulates arriving at the interface.

3.3. Comparison between the regeneration, rain and accumulation rates of Ba

At steady-state, the rain rates of particulate matter carrying Ba to the sediment must balance Ba regeneration and accumulation rates. In the context of such comparative studies, it is more meaningful to derive regional estimates for the Ba fluxes than to treat each station separately. Thus, the cores were divided into three groups: a high flux and high productivity group between $2°N$ and $2°S$, which includes 3 stations at $2°N$, the equator and $2°S$; a group representing intermediate fluxes, which comprises stations $9°N$, $5°N$ and $5°S$; and a low flux, low productivity group represented by station $12°S$. Mean regeneration (pore-water flux), rain (to the sediment), and accumulation (in the sediment) rates of Ba for each zone are defined and listed in Table 4. The Ba rain rates were determined from year-long sediment trap deployments made in 1992–93 [15]. The Ba accumulation rates were estimated using sediment mass accumulation rates from DeMaster and Pope [34], and the total Ba content of the sediments measured by complete dissolution of sediment samples (Table 4, footnote). The three zonal regeneration rates (mean benthic pore-water fluxes for each group of stations), calculated from the corrected for hydrostatic pressure displacement given in Table 3, are given in Table 4.

A comparison between the estimated benthic Ba fluxes and the Ba rain rates to the sea floor as measured by sediment traps shows that, in most cases, they are similar in magnitude (Table 4). This is contrary to expectation; the rain rates should equal the sum of the accumulation and regeneration. Similar high benthic fluxes compared to rain rates have been observed before for both organic carbon and biogenic silica [37]. The consistency of the discrepancies, between the sediment trap rain rates and that calculated from sediment accumulation and regeneration rates, at all stations suggest they might be real; a plausible reason for the discrepancy is that sediment trap data, which provide average fluxes over one year, may not adequately represent the average flux to the site at time scales represented by the benthic

processes of regeneration, particularly of accumulation rates which typically average over thousands of years [44]. The high interannual variability that is found in long term trap deployments attests to the limitation of comparing yearly sediment trap fluxes with benthic processes [45,46]. Alternatively, there may be some near-bottom focused redeposition of sediments, particularly in the region near the equator. Using the calculated fluxes given in Table 4, it is possible to asses the recycling efficiency (RE = 1 − burial efficiency) of Ba in oxic Equatorial Pacific sediments. The recycling efficiency is defined as the ratio of the Ba regeneration (pore water) flux to the calculated total Ba input to the sediment. The Ba input term is the sum of the regeneration and the Ba burial fluxes. The Ba burial rate in the central Equatorial Pacific was estimated using sediment mass accumulation rates from DeMaster and Pope [34] and the total Ba content of the sediment measured in the present study (Table 4). The resulting calculated recycling efficiency for Ba in sediments of the central Equatorial Pacific is about 70% (Table 4) thus, the Ba burial efficiency is approximately 30%.

As mentioned above, the pore-water Ba profiles also indicate a Ba flux from the subsurface maximum into the sediment. The downward fluxes of Ba for the Equatorial Pacific sediments were estimated assuming linear gradients between the pore-water Ba concentration maxima at 0.3 cm and the dissolved Ba concentration at 2 cm down-core, the depth at which the pore-water Ba concentrations become rather constant. Calculated fluxes into the sediments for each zone are given in Table 4. These fluxes are between 10% and 20% of the benthic flux (out of the sediment) and may account for up to 50% of the total Ba accumulating in these sediments. These results suggest that some of the total Ba in these sediments is recycled during early diagenesis. The exact phase in which this diagenetic Ba precipitates cannot be determined from data collected in the present study: it could be adsorbed on mineral surfaces, co-precipitated with Fe–Mn oxyhydroxides or precipitated as barite. This, however, would not influence the usefulness of barite as a suggested new phase that records seawater chemistry and isotopic composition. If Ba reprecipitates as barite in the upper few centimeters of the sediment, where the pore-water is in diffusive communication with bot-

Table 4
Ba rain accumulation and recycling rates in the central Equatorial Pacific

Core numbers	Mean benthic pore-water flux [a] (nmol cm^{-2} yr^{-1})	Mean benthic lander flux [b] (nmol cm^{-2} yr^{-1})	Accumulation rate in sediments [c] (nmol cm^{-2} yr^{-1})	Expected Ba rain rate [d] (nmol cm^{-2} yr^{-1})	Sediment trap flux [e] (nmol cm^{-2} yr^{-1})	Recycling efficiency [f] (%)	Flux into sediments [g] (nmol cm^{-2} yr^{-1})
2°S, Eq, 2°N	31 ± 7	30	17	48	24 ± 12	69	4
5°S, 5°N, 9°N	14 ± 2	15	7	21	15 ± 7	67	3
12°S	6 ± 1	5	2	8	9 ± 2	75	

[a] Calculated using the mean dissolved Ba fluxes, corrected for hydrostatic pressure displacement from Table 3 for the appropriate stations. [b] Ba benthic chamber fluxes from McManus (pers. commun.). [c] Holocene Ba accumulation rate in the sediment calculated from the weight percent Ba in the sediment; 1600, 800, 1500 ppm for the high, intermediate and low productivity areas and sediment accumulation rates of 1.5, 1.2, and 0.17 g cm^{-2} kyr^{-1}, respectively [34]. [d] Ba rain flux, the sum of the pore water Ba regeneration flux and Ba accumulation in the sediment. [e] Ba sediment trap flux from Dymond and Collier [15]. [f] Defined as the pore water benthic Ba flux divided by the total Ba rain rate. [g] Calculated using a linear gradient from 0.3 cm to 2 cm in the sediment.
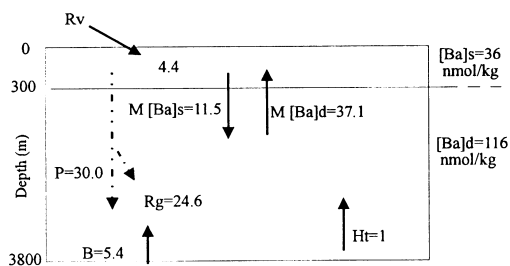
Fig. 3. Box model of the marine cycle of Ba. All fluxes shown are in nmol cm^{-2} yr^{-1}. M is the water exchange rate, which is equal to 3.2 m yr^{-1} [42]; Rv is the river flux [47]; Ht is the hydrothermal flux [48]; [Ba]s is the mean surface water Ba concentration; [Ba]d is the mean deep water Ba concentration [12,42]; P, Rg and B are the particulate, regeneration and burial fluxes respectively, these values were calculated assuming steady-state.

tom seawater, the precipitated barite will record the contemporaneous bottom water geochemistry (i.e., the seawater Sr isotope ratio) as well as other important geochemical paleo-oceanographic parameters.

3.4. Benthic Ba fluxes and the oceanic Ba cycle

To check the consistency between the Ba regeneration fluxes calculated in this study and those derived from mass balance considerations of the oceanic Ba cycle, a two-box (surface and deep waters) mixing model of the ocean was constructed. A schematic representation of the model in Fig. 3, is based on the following assumptions and data: (1) the Ba distribution in the ocean is at steady-state; (2) the mean river flux (Rv) of Ba to surface waters is 4.4 nmol cm^{-2} yr^{-1} [47]; (3) the hydrothermal input (Ht) to the bottom water is 1 nmol cm^{-2} yr^{-1} [48]; (4) the surface water box has a depth of 300 m and an average Ba concentration ([Ba]$_s$) of 36 nmol kg^{-1} [42]; (5) the deep water box has a depth of 3500 m (300–3800 m) and an average Ba concentration ([Ba]$_d$) of 116 nmol kg^{-1} [42]; and (6) the vertical exchange rate between deep and surface water (M) is 320 cm yr^{-1} (corresponding to a deep water residence time of 1100 yr). The resulting upwelling Ba flux to the surface box is therefore:

$$[Ba]_d(M) = 37.1 \text{ nmol cm}^{-2} \text{yr}^{-1} \qquad (3)$$

and the downwelling flux is:

$$[Ba]_s(M) = 11.5 \text{ nmol cm}^{-2} \text{yr}^{-1} \qquad (4)$$

Combining Eq. (5) with the river input, the Ba input rate to the surface water can be described as:

$$[Ba]_d(M) + Rv = 41.5 \text{ nmol cm}^{-2} \text{yr}^{-1} \qquad (5)$$

Similarly, combining Eq. (5) and Eq. (4) the particulate flux to the deep box (P) that has to be exported from the surface box can be expressed as:

$$P = [Ba]_d(M) + Rv - [Ba]_s(M)$$
$$= 30.0 \text{ nmol cm}^{-2} \text{yr}^{-1} \qquad (6)$$

In order to maintain steady state, the input of barium to the ocean must be balanced by its burial in the sediment, resulting in a burial rate (B) equivalent to:

$$B = Rv + Ht = 5.4 \text{ nmol cm}^{-2} \text{yr}^{-1} \qquad (7)$$

The percentage of particulate Ba falling into deep water that survives dissolution can be expressed as:

$$\% = B/P \times 100 \qquad (8)$$

Accordingly, ~ 18% of the particulate barium falling into the deep water survives dissolution and 82% is regenerated.

Pore-water data presented above suggest that a significant fraction of Ba regeneration occurs within a few millimeters of the sediment–water interface and is especially high in areas of high productivity. Mass balance calculations using the two-box model of the ocean described above are in agreement with such a scenario and indicate that a high regeneration rate of Ba (~ 80%, which includes regeneration in the water column and at the sediment) is required to balance the oceanic Ba budget. This includes both regeneration in the water column and at the sediment surface, benthic fluxes measured here indicate that much of this regeneration occurs in the sediment. Beside the equatorial divergence zones, areas of high productivity include near-shore upwelling regions and high latitude areas. Equatorial divergence high productivity zones account for approximately 26% of the oceanic sea floor [49] and, according to this study, should have a mean Ba benthic flux of around 30 nmol cm^{-2} yr^{-1}. These areas provide a substantial fraction of the benthic regenerated Ba (~ 37%). Near-shore upwelling and high latitude areas com-

pose 13% of the ocean and have a somewhat higher benthic Ba flux of about 55 nmol cm^{-2} yr^{-1} [23], providing another 34% of the regenerated Ba flux. The remaining 61% of the ocean floor, with a benthic Ba flux close to 10 nmol cm^{-2} yr^{-1}, provides less than 30% of the total Ba flux to the ocean.

4. Summary

1. Flux estimates derived from high resolution pore-water profile studies at in situ temperature, when corrected for pressure displacement effects, are comparable with those acquired in situ, therefore could be reliably used for flux and early diagenesis regeneration studies.
2. Benthic fluxes of dissolved Ba from oxic sediments in the pelagic environment are about 30 nmol cm^{-2} yr^{-1} in areas of high productivity and less than 10 nmol cm^{-2} yr^{-1} elsewhere; these fluxes are much higher than previously estimated.
3. Beneath high productivity areas most of the Ba regeneration occurs in the upper few millimeters of sediment.
4. The zonal distribution of the Ba benthic fluxes in the equatorial region suggests higher benthic fluxes in areas with higher biological productivity.
5. The Ba preservation in the sediment is about 30% (regeneration 70%), which is consistent with oceanic Ba mass balance calculations.

Acknowledgements

References

[1] D.W. Lea, Constraints on the alkalinity and circulation of glacial circumpolar deep water from benthic foraminiferal barium, Global Biogeochem. Cycles 7, 695–710, 1993.

[2] D.W. Lea, G.T. Shen and E.A. Boyle, Corallin barium records temporal variability in equatorial upwelling, Nature 340, 373–376, 1989.

[3] B. Schmitz, Barium, Equatorial high productivity, and the wandering of the Indian continent, Paleoceanography 2, 63–77, 1987.

[4] G.B. Shimmield, N.B. Price and A.A. Kahn, The use of Th-230 and Ba as indicators of paleoproductivity over a 300 Kyr time scale — Evidence from the Arabian Sea, Chem. Geol. 70, 112, 1988.

[5] J. Dymond, E. Suess and M. Lyle, Barium in deep sea sediments: A geochemical proxy for paleoproductivity, Paleoceanography 7, 163–181, 1992.

[6] J.K.B. Bishop, The barite–opal–organic carbon association in oceanic particulate matter, Nature 331, 341–343, 1988.

[7] F. Dehairs, W. Baeyems and L. Goeyens, Accumulation of suspended barite at mesopelagic depths and export production in the Southern Ocean, Science 258, 1332–1335, 1992.

[8] A. Paytan, M. Kastner, E.E. Martin, J.D. Macdougall and T. Herbert, Marine barite as a monitor of seawater strontium isotope composition, Nature 366, 445–449, 1993.

[9] M. Cane, Oceanographic events during El-Nino, Science 222, 1189–1195, 1983.

[10] F.P. Chavez and R.T. Barber, An estimate of new production in the equatorial Pacific, Deep-Sea Res. 34, 1229–1243, 1987.

[11] K. Wolgemuth and W.S. Broecker, Barium in sea water, Earth Planet. Sci. Lett. 8, 372–378, 1970.

[12] L.H. Chan, J.M. Edmond, R.F. Stallard, W.S. Broecker, Y.C. Chung, R.F. Weiss and T.L. Ku, Radium and barium in GEOSECS stations in the Atlantic and Pacific, Earth Planet. Sci. Lett. 32, 258–267, 1976.

[13] M.P. Bacon and J.M. Edmond, Barium at GEOSECS III in the Southwest Pacific, Earth Planet. Sci. Lett. 16, 66–74, 1972.

[14] D.W. Lea and E.A. Boyle, Barium content of benthic foramenifera controlled by bottom water composition, Nature 338, 271–274, 1989.

[15] J. Dymond and R. Collier, Particulate barium fluxes and their relationships to biological productivity, Deep-Sea Res., in press.

[16] T.J. Chow and E.D. Goldberg, On the marine geochemistry of barium, Geochim. Cosmochim. Acta 20, 192–198, 1960.

[17] R.W. Collier and J.M. Edmond, The trace elements geochemistry of marine biogenic particulate matter, Prog. Oceanogr. 13, 113–199, 1984.

[18] F. Dehairs, R. Chesselet and J. Jedwab, Discrete suspended particles of barite and the barium cycle in the open ocean, Earth Planet. Sci. Lett. 49, 529–550, 1980.

[19] R.E. Bernstein, R.H. Byrne, P.R. Betzer and A.M. Greco, Morphologies and transformations of celestite in seawater:

The role of acantharians in the strontium and barium geo-chemistry, Geochim. Cosmochim. Acta 56, 3273–3279, 1992.

[20] J.S. Hanor, Barite saturation in sea water, Geochim. Cosmochim. Acta 33, 894–898, 1969.

[21] T.M. Church and K. Wolgemuth, Marine barite saturation, Earth Planet. Sci. Lett. 15, 35–44, 1972.

[22] K.K. Falkner, G.P. Klinkhammer, T.S. Bowers, J.F. Todd, B.L. Lewis, W.M. Landing and J.M. Edmond, The behavior of barium in anoxic marine waters, Geochim. Cosmochim. Acta 57, 537–554, 1993.

[23] J. McManus, W.M. Berelson, G.P. Klinkhammer, T.E. Kilgore and D.E. Hammond, Remobilization of barium in continental margin sediments, Geochim. Cosmochim. Acta 58, 4899–4907, 1994.

[24] G.P. Klinkhammer and L.H. Chan, Determination of barium in marine waters by isotope dilution inductively coupled plasma mass spectrometry, Anal. Chim. Acta 232, 323–329, 1990.

[25] G.P. Klinkhammer, D.T. Heggie and D.W. Graham, Metal diagenesis in oxic marine sediments, Earth Planet. Sci. Lett. 61, 211–219, 1982.

[26] H. Brumsack and J.M. Gieskes, Interstitial water trace metal chemistry of laminated sediments from the Gulf of California, Mexico, Mar. Chem. 14, 89–106, 1983.

[27] E. Suess, P.J. Muller, H.S. Powell and C.E. Reimers, A closer look at nitrification in pelagic sediments, Geochem. J. 14, 129–137, 1980.

[28] W.M. Berelson, D.E. Hammond, D. O'Neill, X-M. Xu, C. Chin and J. Zukin, Benthic fluxes and pore water studies from sediments of the central equatorial north Pacific: Nutrient diagenesis, Geochim. Cosmochim. Acta 54, 3001–3012, 1990.

[29] D.E. Hammond, J. McManus, W. Berelson, T. Kligore and R. Pope, Early diagenesis of organic material in Equatorial Pacific sediments: Stochiometry and kinetics, Deep-Sea Res., in press.

[30] C. Monnin and C. Galinier, The solubility of celestite and barite in electrolyte solutions and natural waters at 25°C: a thermodynamic study, Chem. Geol. 71, 283–296, 1988.

[31] A.R. Felmy, R. Dhanpat and J.E. Amonette, The solubility of barite and celestite in sodium sulfate: evaluation of thermodynamic data, J. Solution Chem. 19, 175–185, 1990.

[32] R.A. Berner, Early Diagenesis: A Theoretical Approach, 241 pp., Prinston University Press, Prinston, N.J., 1980.

[33] C.R. Smith, S.P. Garner, D.J. Hoover and R.H. Pope, Macrobenthos, mechanisms of bioturbation, and carbon flux proxies at the abyssal seafloor along the JGOFS Equatorial Pacific transect, EOS 75, 70, 1994.

[34] D.J. DeMaster and R.H. Pope, C-14 chronologies, biogenic accumulation rates and sediment mixing coefficients along the equatorial Pacific JGOFS transect, The Oceanographic Society, 4th Annu. Meet., abstract, 1994.

[35] J. McManus, W.M. Berelson, D.E. Hammond and T.E.

Kligor, Early diagenesis of biogenic opal: Dissolution rates, kinetics, and paleoceanographic implications, Deep-Sea Res., in press.

[36] Y.H. Li and S. Gregory, Diffusion of ions in sea water and in deep-sea sediments, Geochim. Cosmochim. Acta 33, 703–714, 1974.

[37] R.W. Martin, M. Bender, M. Leinin and J. Orchard, Benthic organic carbon degradation and biogenic silica dissolution in the central equatorial Pacific, Deep-Sea Res. 38, 1481–1516, 1991.

[38] K.A. Fanning and M.E.Q. Pilson, Interstitial silica and pH in marine sediments: Some effects of sampling procedures, Science 173, 1228–1231, 1971.

[39] J.W. Murray, S. Emerson and R. Jahnke, Carbonate saturation and the effect of pressure on the alkalinity of interstitial waters from the Guatemala Basin, Geochim. Cosmochim. Acta 44, 963–967, 1980.

[40] R.A. Jahnke, S.R. Emerson, C.E. Reimers, J. Schuffert, K. Ruttenberg and D. Archer, Benthic recycling of biogenic debris in the eastern tropical Atlantic Ocean, Geochim. Cosmichim. Acta 53, 2947–2960, 1989.

[41] D.A. Anati, Advection and diffusion in marine sediments: DSDP site 374 Eastern Mediterranean as an example, Earth Planet. Sci. Lett. 128, 575–589, 1994.

[42] Y.H. Li, T.L. Ku, G.G. Mathieu and K. Wolgemuth, Barium in the Antarctic Ocean and implications regarding the marine geochemistry of Ba and Ra-226, Earth Planet. Sci. Lett. 19, 267–285, 1973.

[43] F.C. Dobbs, Bacterial densities and microbial biomass along the Equatorial Pacific transect, EOS 75, 70, 1994.

[44] J. Dymond and M. Lyle, Flux comparisons between sediments and sediment traps in the eastern tropical Pacific: Implications for atmospheric CO_2 variations during the Pleistocene, Limnol. Oceanogr. 30, 699–712, 1985.

[45] W.G. Deuser, Seasonality of particle fluxes in the ocean's interior, in: Global Ocean Flux Study: Proceedings of a Workshop, pp. 221–236, Natl. Acad. Press, Washington, DC, 1984.

[46] S. Honjo, Study of ocean fluxes in time and space by bottom-tethered sediment trap arrays: A recommendation, in: Global Ocean Flux Study: Proceeding of a Workshop, pp. 305–324, Natl. Acad. Press, Washington, DC, 1984.

[47] J.M. Edmond, E.D. Boyle, D. Drummond and G. Grant, Desorption of Ba in the plume of the Zaire River, Neth. J. Sea Res. 12, 324–328, 1978.

[48] K.L. Von Damm, J.M. Edmond, C.I. Measures and B. Grant, Chemistry of submarine hydrothermal solutions at 21°N, East Pacific Rise, Geochim. Cosmochim. Acta 49, 2197–2220, 1985.

[49] O.I. Koblents-Mishke, V.V. Vokovinski and Y.G. Kabanova, Plankton primary production of the world ocean, in: Scientific Exploration of the South Pacific, pp. 183–193, Natl. Acad. Sci., Washington, DC, 1970.